The Arf activator Gea2p and the P-type ATPase Drs2p interact at the Golgi in *Saccharomyces cerevisiae*

Sophie Chantalat[2], Sei-Kyoung Park[1], Zhaolin Hua[3], Ke Liu[3], Renée Gobin[2], Anne Peyroche[2], Alain Rambourg[2], Todd R. Graham[3] and Catherine L. Jackson[1,*]

[1]Cell Biology and Metabolism Branch, National Institute of Child Health and Human Development, National Institutes of Health, Bethesda, MD 20892-5430, USA
[2]Departement de Biologie Joliot-Curie, CEA/Saclay, Gif-sur-Yvette F-91191, France
[3]Department of Biological Sciences, Vanderbilt University, Nashville, TN 37235, USA
*Author for correspondence (e-mail: cathyj@helix.nih.gov)

Accepted 19 September 2003
Journal of Cell Science 117, 711-722 Published by The Company of Biologists 2004
doi:10.1242/jcs.00896

Summary

Arf GTPases regulate both the morphological and protein sorting events that are essential for membrane trafficking. Guanine nucleotide exchange factors (GEFs) specific for Arf proteins determine when and where Arf GTPases will be activated in cells. The yeast Gea2p Arf GEF is a member of an evolutionarily conserved family of high molecular mass Arf GEFs that are peripherally associated with membranes. Nothing is known about how these proteins are localized to membranes, and few direct binding partners have been identified. In yeast, Gea2p has been implicated in trafficking through the Golgi apparatus and in maintaining Golgi structure. A major function of the Golgi apparatus is the packaging of cargo into secretory granules or vesicles. This process occurs through a series of membrane transformation events starting with fenestration of a saccular membrane, and subsequent remodeling of the fenestrated membrane into a mesh-like tubular network. Concentration of secretory cargo into nodes of the tubular network leads to enlargement of the nodes, which correspond to forming vesicles/granules, and thinning of the surrounding tubules. The tubules eventually break to release the secretory vesicles/granules into the cytoplasm. This process is highly conserved at the morphological level from yeast to mammalian cells. Drs2p, a multi-span transmembrane domain protein and putative aminophospholipid translocase, is required for the formation of a class of secretory granules/vesicles in yeast. Here we show that Drs2p interacts directly with Gea2p, both in vitro and in vivo. We mapped the domain of interaction of Drs2p to a 20-amino-acid region of the C-terminal cytoplasmic tail of the protein, adjacent to a region essential for Drs2p function. Mutations in Gea2p that abolish interaction with Drs2p are clustered in the C-terminal third of the Sec7 domain, and are important for Gea2p function. We characterize one such mutant that has a thermosensitive phenotype, and show that it has morphological defects along the secretory pathway in the formation of secretory granules/vesicles.

Key words: Arf guanine nucleotide exchange factor (GEF), Arf GTPase, Aminophospholipid translocase, Golgi apparatus, Secretory vesicles, Secretory granules, Membrane dynamics

Introduction

The Arf GTPases and their regulators play an important role in protein trafficking and organelle structure in eukaryotic cells. Like all small G proteins, Arf (for **A**DP-**r**ibosylation **f**actor) exists in two states, depending on the bound guanine nucleotide. In its GDP-bound form, Arf is largely soluble, whereas Arf-GTP is tightly membrane bound. Exchange of GDP for GTP is carried out by guanine nucleotide exchange factors (GEFs), all of which possess a Sec7 domain, a 200-amino-acid region that alone is able to carry out the exchange reaction in vitro (Jackson and Casanova, 2000). There are at least five Arf GEFs in *Saccharomyces cerevisiae*, and 15 in humans (Jackson, 2004). All of the Sec7 domain GEFs are peripherally associated membrane proteins. Some family members have a lipid-binding pleckstrin homology (PH) domain downstream of their Sec7 domain that mediates membrane association (Jackson et al., 2000; Randazzo et al., 2001). We are studying yeast Gea1p and Gea2p, members of a subfamily of Arf GEFs that also includes human GBF1 and *Arabidopsis* GNOM (Jackson and Casanova, 2000). These GEFs are large (≥150 kDa), and localize to the Golgi (Gea1p, Gea2p, GBF1) or to endosomes (GNOM) (Chantalat et al., 2003; García-Mata et al., 2003; Geldner et al., 2003; Spang et al., 2001; Zhao et al., 2002). These proteins have no obvious PH domain or other localization determinants, and the mechanism of their targeting to membranes is unknown.

Upon activation by an Arf GEF, Arf-GTP interacts with a number of effectors. The best-studied of these are coat proteins, large cytosolic complexes that are recruited to membranes by Arf-GTP. The coat complex COPI is recruited to early Golgi membranes, whereas clathrin/adaptor and GGA coats are recruited to late Golgi and endosomal membranes (Robinson and Bonifacino, 2001). Arf-GTP also activates lipid-modifying enzymes, such as phospholipase D and phosphatidylinositol 4-phosphate-5-kinase (Donaldson and Jackson, 2000). Hence activation of Arf leads to changes in both the protein and lipid composition of the membrane on which it is located. Most of the well-studied components

regulating trafficking through the Golgi apparatus are peripherally associated proteins (Arf, Arf GEFs and coats), and only a few transmembrane proteins have been implicated. One such protein is Drs2p, a 10-span transmembrane P-type ATPase that functions as a putative aminophospholipid translocase (Tang et al., 1996). Mutant alleles of *DRS2* were recovered in an *arf1* synthetic lethal screen, the first result to implicate Drs2p in protein transport (Chen and Graham, 1998). *drs2Δ* cells are viable, but have a cold-sensitive growth phenotype. At the non-permissive temperature, drs2*Δ* cells have a defect in clathrin-mediated trafficking events at the late Golgi (Chen et al., 1999). Drs2p is required for the formation of a class of secretory vesicles/granules that also require clathrin for their biogenesis (Gall et al., 2002).

Protein transport through the secretory pathway is accompanied at the morphological level by a series of membrane transformation events. A region of the endoplasmic reticulum (ER) becomes fenestrated, then reorganizes into a tubular network of hexagonal or pentagonal mesh. In yeast, these tubular networks remain scattered throughout the cytoplasm and make up the Golgi apparatus. In a wild-type yeast cell, approximately 20-30 Golgi tubular networks are present in a given cell. Secretory granules/vesicles arise from these tubular networks in a process that is highly conserved from yeast to mammals (Rambourg and Clermont, 1990; Rambourg et al., 2001). At the nodes of the meshes, the secretory cargo becomes concentrated, and each node enlarges into a forming secretory granule/vesicle as the material in the surrounding tubules is depleted. Finally, the thinning tubules break to release the secretory granule into the cytoplasm. A major challenge is to determine how these membrane transformation events are accomplished at the molecular level. Previous results demonstrate that Arf and its activators, the Arf GEFs, play an important role in these membrane transformation events (Deitz et al., 2000; Peyroche et al., 2001).

We demonstrate that Drs2p and the Arf GEF Gea2p interact directly and functionally in yeast cells. We have mapped the interaction sites on both proteins, and identified mutations in each protein that abolished interaction. One such mutation in Gea2p was characterized and although trafficking defects are mild, this mutant exhibits significant morphological defects along the secretory pathway in the formation of secretory granules/vesicles.

Materials and Methods

Media, strains and plasmids

Standard yeast genetic techniques and media were used (Sherman et al., 1979). Plasmids and strains used in this study are listed in Tables 1 and 2. SCY020-9-4 was generated by mating SEY6210 *drs2Δ::URA3* with CJY049-2-1, sporulation of the resulting diploid, and tetrad dissection. Strains CJY088 and CJY089 were constructed from strains SEY6210 and SEY6210 *drs2Δ::URA3*, respectively, using pFA6a-3HA-TRP1 (Longtine et al., 1998), in which the chromosomal copy of GEA2 was fused at its 3′ end with a DNA fragment encoding three tandem copies of the HA epitope. Strains CJY090 and CJY091 were constructed by integrating a plasmid encoding three tandem copies of EGFP at the 3′ end of *GEA2* into strains SEY6210 and SEY6210 *drs2Δ::URA3*, respectively, using an integrative vector derived from a triple EGFP plasmid kindly provided by Ben Glick. *DRS2* C-terminal tail deletion mutant plasmids were generated by PCR amplification of the different regions of the *DRS2* C terminus, which were used to replace the *Nco*I/*Mlu*I region of pRS315-*DRS2*. *DRS2* internal deletion mutants were generated from the truncation mutants with C-terminal sequences added as a *Mlu*I/*Sal*I PCR fragment.

Two-hybrid analysis

We cloned the Sec7 domain of Gea2p (amino acids 557-769) into pGBT9 to create a fusion with the DNA binding domain of Gal4p (pSC2). This fusion protein showed a specific interaction with the dominant negative Δ17-ArfT31N fused to the activation domain of Gal4p. We used the ArfT31N mutant because it binds to GEFs with a higher affinity than wild-type Arf. Full-length Gea1p cloned into the Gal4p DNA-binding domain vector pASΔ (Flores et al., 1999) also interacted with Δ17-ArfT31N. The two-hybrid screen with pSC2 as bait was performed as previously described (Flores et al., 1999). We identified 146 positive clones out of a total of 1.23×10^7 transformants screened. The C-terminal region of the Drs2p was found six times. The region corresponding to amino acids 1230-1355 of Drs2p was identified in a two-hybrid library plasmid found four times; two other library plasmids encoded regions of Drs2p starting at amino acids 1198 and 1213.

For the reverse two-hybrid screen using the *DRS2* C-terminal tail, random mutations were introduced into pDHS279 by performing PCR under conditions designed to reduce the fidelity of the polymerase (addition of 50 μM $MnCl_2$). A gap was introduced into the pDHS279 plasmid. The PCR product extended to 120 and 60 base pairs past the 5′ and 3′ ends of the gap, respectively. The mutagenized PCR product and gapped vector were used to transform Y190 cells that carried the bait plasmid pSC2. Transformants were replicated onto synthetic medium plates lacking histidine and containing 25 mM 3-AT and assayed for β-galactosidase activity directly. Approximately 6500 transformants were screened and 150 white or light blue colonies identified. Twenty percent of these were found to be full-length; the remainder were truncations due to introduction of stop codons or frameshift mutations. Plasmids expressing a full-length *DRS2* C-terminal tail were rescued from yeast and inserts were sequenced to identify mutations. Given that a part of the Gal4p DNA binding domain was subjected to mutagenesis, the *DRS2* fragment from each pDHS279 mutant was subcloned into pACT2 in order to verify that loss of interaction was the result of a *DRS2* point mutation. Mutants that gave only a partial loss of interaction, that had multiple mutations, or those caused by mutations elsewhere in the plasmid than in the DRS2 portion, were discarded. Nine single mutants that caused complete or almost complete loss of interaction by two-hybrid analysis remained and were used to define the Gea2p binding site on Drs2p. A similar method was used for the reverse two-hybrid screen carried out using pSC2, except that 2-hybrid strain AH109 was used and loss of interaction mutants were scored as red *ade2*– clones.

In vitro binding assay

A fragment encoding amino acids 1230-1355 of Drs2p was cloned into *E. coli* expression vector pRSET5d (Schoepfer, 1993) for in vitro transcription-translation, and into a derivative of pRSET5d to generate an HA-tagged fusion protein. Codons 557-769 of the Gea2p protein (the same Sec7 domain region as in the 2-hybrid construct) were cloned into the same vectors. For expression of proteins in *E. coli*, transformed BL21(DE3) cells were grown at 30°C in LB (Luria Bertani) medium supplemented with ampicillin (500 μg/ml), chloramphenicol (34 μg/ml) and 1 M sorbitol. Expression of recombinant protein was induced at an OD_{600} of 0.5 with 1 mM isopropyl-β-D-thiogalactopyranoside (IPTG). Cells were shaken for 6 hours at 24°C, collected and resuspended in IP buffer (Tris pH 7.5 50 mM, $MgCl_2$ 5 mM, potassium acetate 100 mM, DTT 1 mM, NP40 0.1%, glycerol 15%) supplemented with complete protease inhibitor

Table 1. Plasmids used in this study

Plasmid	Description	Reference
pSC2	pGBT9-*GEA2(aa 557-769)*	This study
pSC59-2	pASΔ-*GEA1*	This study
pSC8	pRSET5d-*GEA2(aa 557-769)*	This study
pSC9	pRSET5d-*His6-HA-GEA2(aa 557-769)*	This study
pSC10	pRSET5d-*DRS2(aa 1230-1355)*	This study
pSC11	pRSET5d-*His6-HA-DRS2(aa 1230-1355)*	This study
pSC12	pRSET5d-*DRS2(aa 1230-1305)*	This study
pSC13	pRSET5d-*DRS2(aa 1305-1355)*	This study
pGMS3	*2μ, URA3, GEA2*	This study
pGMS3-HA	*2μ, URA3, GEA2-3x HA*	This study
pSKP1	*CEN, URA3, GEA2*	This study
pRS315-DRS2	*CEN, LEU2, DRS2*	(Chen et al., 1999)
pRS425-DRS2	*2μ, LEU2, DRS2*	(Chen et al., 1999)
pCM116C	*CEN, LEU2, TPIprom-KEX2-HA*	(Mullins and Bonifacino, 2001)

cocktail (Boehringer Mannheim) and 1 mM PMSF. Cells were lysed by two cycles of freezing and thawing in liquid nitrogen. Lysozyme (20 μg/ml) and benzonase (250 U/ml) were added and the suspension was incubated for 30 minutes at 30°C. Crude extract was briefly sonicated and centrifuged at 100,000 ***g*** at 4°C for 1 hour. The S100 fraction with or without HA-tagged Gea2p Sec7 domain was passed three times over a column of protein G Sepharose (Pharmacia) coated with anti-HA antibodies (12CA5), equilibrated in IP buffer with 1% (w/v) non-fat milk. The beads were extensively washed with IP buffer with 1% (w/v) non-fat milk. ^{35}S-labeled proteins were synthesized in a wheatgerm extract (Promega) supplemented with T7 RNA polymerase (Promega, Madison, WI), [^{35}S]methionine (0.8 mCi/ml) and 1 μg of purified plasmid encoding protein fragments. The Drs2p C terminus derived from an in vitro transcription-translation reaction was passed over the column containing HA-tagged Gea2 Sec7 domain or the control column. After extensive washing with IP buffer, proteins were eluted in 2× SDS Laemmli buffer. Proteins were subjected to SDS-PAGE and analyzed by Coomassie Blue staining and western blotting using anti-HA antibodies and by autoradiography on BiomaxMS films (Amersham, Buckinghamshire, UK). Approximately 10% of the total reaction product was retained on the Gea2-HA column. The reverse experiment, in which ^{35}S-labeled Gea2p Sec7 domain was passed over a column of HA-tagged Drs2p C terminus was performed as described above.

Subcellular fractionation and OptiPrep™ density gradient analysis

Subcellular fractionation and OptiPrep™ density gradient analysis were performed as described by the manufacturer (Axis-Shield PoC, Oslo, Norway). Briefly, 1.0 l liquid cultures of strains CJY088 Gea2-HA and CJY089 *drs2Δ::URA3* Gea2-HA carrying a Kex2-HA plasmid (pCM116C) were grown to mid-logarithmic phase in synthetic medium lacking leucine (SC-LEU; Q-Biogene, Carlsbad, CA). Cells were harvested by centrifugation, converted to spheroplasts and lysed in buffer B (0.2 M sorbitol, 1 mM EDTA, 20 mM Pipes-KOH, pH 6.8). After a clearing spin at 500 ***g***, the lysates were spun at 100,000 ***g*** for 20 minutes at 4°C. The P100 fraction was resuspended in buffer B, loaded onto a 10 ml OptiPrep™ gradient (0-60%) and spun at 100,000 ***g*** for 16 hours at 4°C. Fourteen fractions were collected from the top of the gradient. Aliquots were loaded onto SDS-polyacrylamide gels and subjected to immunoblot analysis. Mouse monoclonal HA.11 anti-hemagglutinin (anti-HA) antibodies were from Covance (Princeton, NJ), and mouse monoclonal antibodies against the vacuolar ATPase (100 kDa subunit), Pep12p and Dpm1p were purchased from Molecular Probes (Eugene, OR). Rabbit polyclonal antibodies against Drs2p have been described previously (Chen et al., 1999). Anti-Sec61p, anti-Sed5p and anti-Sec22p antisera were generous gifts from Randy Schekman and Gerry Waters.

Cell labeling and immunoprecipation

Pulse-labeling of yeast cells with [^{35}S]methionine and [^{35}S]cysteine, immunoprecipitation and secretion of proteins into the medium were performed as described previously (Peyroche et al., 2001). For co-immunoprecipitation experiments, yeast cells (60 OD_{600} units) were harvested at mid-logarithmic phase and washed once with 10 mM NaN_3 and once with lysis buffer (20 mM Hepes pH 7.2, 100 mM KCl, 5 mM $MgCl_2$ and 1% Triton X-100). Cells were disrupted with acid-washed glass beads (Sigma) in 0.1 ml lysis buffer supplemented with complete protease inhibitor cocktail (Boehringer Mannheim, Germany) and 1 mM Pefabloc (Roche, Basel, Switzerland). The cell lysate was centrifuged twice at 500 ***g*** and the supernatant was then centrifuged at 100,000 ***g*** at 4°C for 1 hour. Cleared lysates were diluted tenfold in lysis buffer lacking Triton X-100 and incubated with 25 μl of protein G-Sepharose (Amersham Pharmacia) coupled to anti-HA antibodies (12CA5) for at least 2 hours at 4°C. The resin was then washed twice with buffer containing 200 mM KCl and 0.1% Triton X-100 and resuspended in 2× SDS-Laemmli sample buffer. Bound proteins were analyzed by SDS-PAGE and immunoblotting.

Microscopy

To visualize cells expressing GFP-tagged proteins, cells were grown to mid-logarithmic phase and concentrated. Images were obtained on an Olympus IX-70 fluorescence microscope with an IMAGO

Table 2. Strains used in this study

Strain	Genotype	Reference
Y190	*MATa gal4Δ gal80Δ his3-Δ200 trp1-901 ade2-101 ura3-52 leu2-3, 112 URA3::GAL->lacZLYS2::GAL->HIS3 cyhR*	S. J. Elledge
C13-ABYS86	*MATα pra1-1 prb1-1 prc1-1 cps1-3 ura3Δ5 leu2-3, 112 his⁻*	(Heinemeyer et al., 1991)
SEY6210	*MATα ura3-52 leu2-3,112 his3Δ200 lys2-801 trp1Δ901 suc2Δ9*	S. Emr
SEY6210*drs2Δ::TRP1*	*MATα ura3-52 leu2-3,112 his3Δ200 lys2-801 trp1Δ901 suc2Δ9 drs2::TRP1*	(Chen et al., 1999)
SEY6210*drs2Δ::URA3*	*MATα ura3-52 leu2-3,112 his3Δ200 lys2-801 trp1Δ901 suc2Δ9 drs2::URA3*	This study
CJY049-2-1	*MATa ura3-52 leu2-3,112 his3Δ200 lys2-801 GEA1 gea2::HIS3*	This study
SCY020-9-4	*MATα ura3-52 leu2-3,112 his3Δ200 lys2-801 GEA1 drs2::URA3 gea2::HIS3*	This study
CJY088	*SEY6210 GEA2-3xHA::TRP1*	This study
CJY089	*SEY6210 drs2Δ::URA3 GEA2-3xHA::TRP1*	This study
CJY090	*SEY6210 GEA2-3xEGFP*	This study
CJY091	*SEY6210 drs2Δ::URA3 GEA2-3xEGFP*	This study
CJY052-10-2	*MATα ura3-52 leu2-Δ1 his3-Δ200 lys2-801ade2-101 trp1-Δ63gea1::HIS3 gea2::HIS3 / pCLJ90 CEN-TRP1-GEA1*	(Peyroche et al., 2001)
CJY092	*MATα ura3-52 leu2-Δ1 his3-Δ200 lys2-801ade2-101 trp1-Δ63gea1::HIS3 gea2::HIS3/pSKP1 CEN-URA3-GEA2*	This study
CJY093	*MATα ura3-52 leu2-Δ1 his3-Δ200 lys2-801ade2-101 trp1-Δ63gea1::HIS3 gea2::HIS3/pCEN-URA3-gea2V698G*	This study

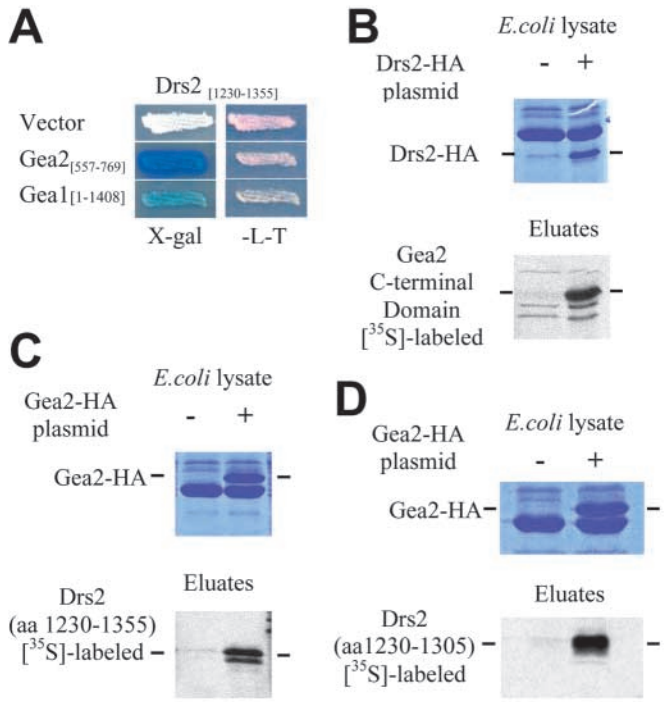

Fig. 1. The Sec7 domain of Gea2p interacts with Drs2p. (A) Yeast two-hybrid strain Y190 carrying the C-terminal region of Drs2p (amino acids 1230-1355) in a two-hybrid prey vector and either the Gea2p Sec7 domain, full-length Gea1p or the two-hybrid bait vector alone were grown on selective medium lacking leucine and tryptophan (–L-T) that selects for each plasmid (right), or on medium containing X-gal (5-bromo-4-chloro-3-indolyl-β-D-galactoside) (left). (B) Drs2-HA was expressed in *E. coli*, and cell lysates loaded onto an anti-HA antibody affinity column. The Sec7 domain of Gea2p was transcribed and translated in vitro in the presence of [^{35}S]methionine. The radiolabeled protein was passed over the Drs2-HA column, and a control column loaded with lysates from cells not expressing Drs2-HA. (C,D) The Gea2 Sec7 domain tagged with HA was expressed in *E. coli* and bound to an anti-HA antibody affinity column. The full-length Drs2p C terminus, amino acids 1230-1355 (C) and two halves, amino acids 1230-1305 (D) and amino acids 1306-1355 (not shown) were radiolabeled in vitro and passed over Gea2 Sec7 domain and control columns. The bound fraction was run on SDS-PAGE gels, which were exposed to film. Coomassie Blue-stained gels of the *E. coli* cell lysates used to prepare each column are also shown.

charge-coupled digital camera controlled by TILLvisION software (T.I.L.L. Photonics, Gräfelfing, Germany). Electron microscopy was performed as described previously (Rambourg et al., 2001) using the reduced osmium fixation method and counterstaining with thiocarbohydrazide-silver proteinate.

Results

Drs2p binds directly to the Sec7 domain of Gea2p

We carried out a two-hybrid screen using the Sec7 domain of Gea2p. One of the candidates we identified was the C-terminal cytoplasmic region of Drs2p (Fig. 1A). Drs2p is a Golgi-localized P-type ATPase and potential aminophospholipid translocase with 10 transmembrane domains (Chen et al., 1999). The region downstream of the final membrane-spanning domain is predicted to face the cytoplasm, and hence could potentially interact with Gea2p, a peripherally associated Golgi membrane protein (Chantalat et al., 2003; Spang et al., 2001). Although a two-hybrid construct expressing the Sec7 domain of Gea1p was not functional, we were able to express full-length Gea1p fused to the DNA-binding domain of Gal4p. Full-length Gea1p was also able to interact with the C terminus of Drs2p (Fig. 1A). To confirm the two-hybrid interaction between Gea2p and Drs2p, we translated the Gea2p Sec7 domain in vitro and expressed the Drs2p C-terminal region (amino acids 1230-1355) in *E. coli*. The Gea2-Sec7 domain was retained on columns loaded with HA-tagged Drs2p (1230-1355), in contrast to the control column lacking HA-Drs2p (Fig. 1B). Similarly, when HA-tagged Gea2-Sec7 domain was loaded onto columns, the C-terminal region of Drs2p (aa 1230-1355) bound specifically (Fig. 1C). To further define the region of interaction, binding of the membrane-proximal and membrane-distal regions of the Drs2p tail were tested. The membrane-proximal region of Drs2p (aa 1230-1305) gave as strong a signal in the in vitro binding assay as the full-length tail (Fig. 1D). The extreme C terminus (aa 1306-1355) of Drs2p did not bind detectably to the column loaded with the Sec7 domain of Gea2 (data not shown), indicating that the binding region is within a 75-amino acid membrane-proximal region of the Drs2p C-terminal domain.

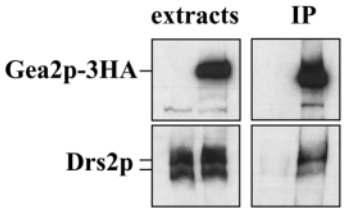

Fig. 2. Co-immunoprecipitation of Gea2p and Drs2p from yeast cells. C13-ABYS86 cells carrying 2μ-*DRS2* (pRS425-*DRS2*) and either 2μ-*GEA2* (pGMS3) or 2μ*GEA2-HA* (pGMS3-HA) were grown to exponential phase and lysates prepared. Gea2p-HA was immunoprecipitated using anti-HA antibodies, and the bound material run on an SDS-polyacrylimide gel and transferred to nitrocellulose. Antibodies against Drs2p were used to probe the blots.

Gea2p and Drs2p interact functionally in yeast cells

To determine if the Gea2p and Drs2p proteins interact in cells, we carried out co-immunoprecipitation experiments. Wild-type cells were transformed with a multicopy 2μ plasmid carrying full-length Drs2p, and either 2μ-Gea2-HA or vector alone. Cell lysates were subjected to immunoprecipitation with anti-HA antibodies, and the presence of Drs2p in the immunoprecipitates was monitored by western blotting using anti-Drs2p antibodies. Drs2p was found in immunoprecipitates from the Gea2-HA-expressing cells, but not in the control, demonstrating that the two proteins are associated in yeast cells (Fig. 2).

Drs2p has been localized to the late Golgi in yeast, and colocalizes with Kex2p (Chen et al., 1999). Gea2p co-localizes with Golgi markers at steady state, as determined by immunofluorescence analysis (Chantalat et al., 2003). We carried out fractionation experiments comparing the localization of Gea2p in a wild type and a *drs2Δ* mutant. We used OptiPrep^{TM} density gradients to separate organelles from a yeast membrane preparation. In these preparations, Gea2-HA was distributed between membrane and cytosolic fractions, with no significant difference between wild-type and *drs2Δ* strains. For the wild-type strain, 64% of Gea2-HA was present

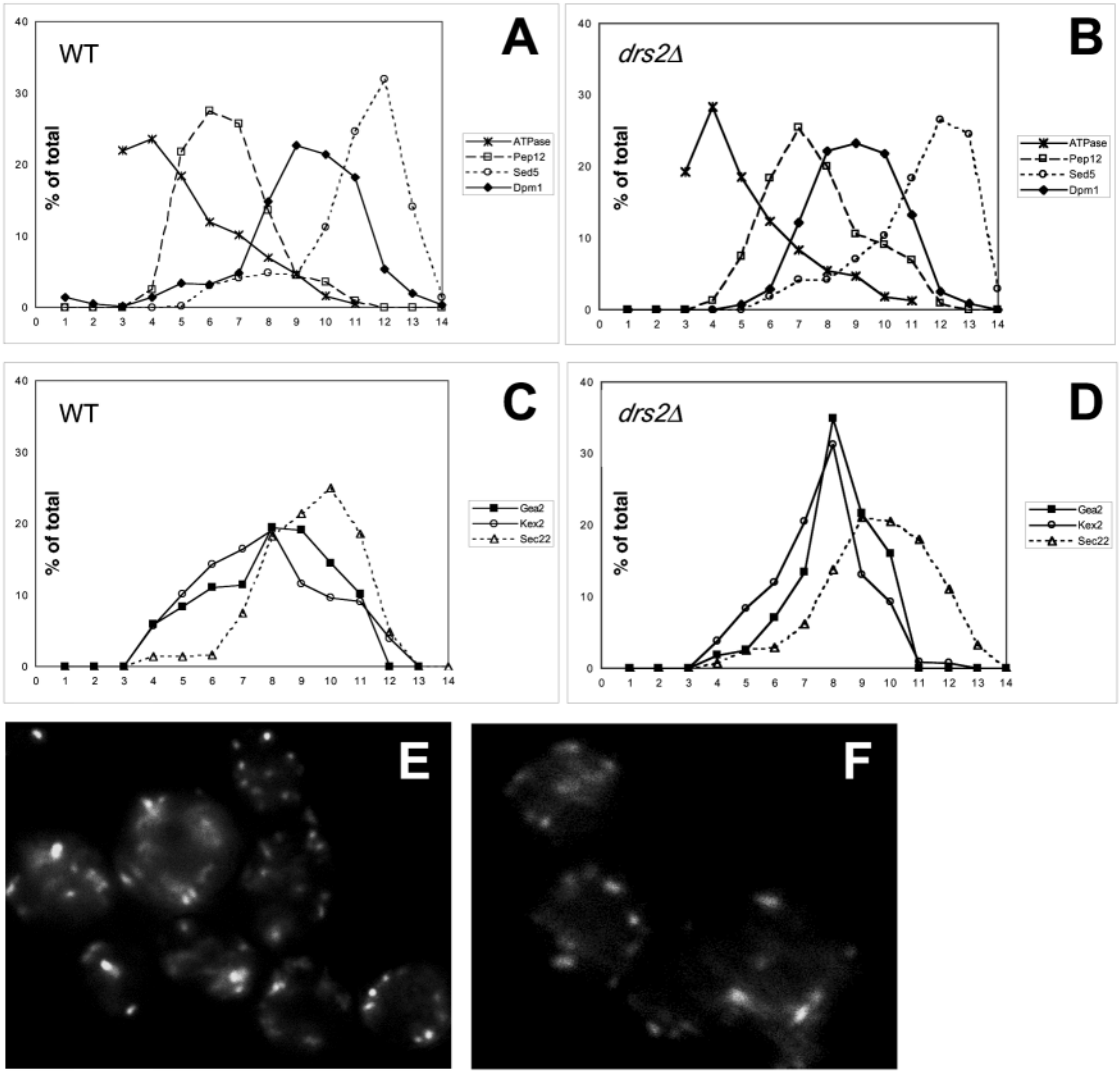

Fig. 3. Localization of Gea2p in wild-type and *drs2Δ* cells. Wild-type CJY088 (A,C) and CYJ089 *drs2Δ* (B,D) cell membrane preparations were fractionated on OptiPrep™ gradients as described in Materials and Methods. Antibodies against different organelle markers were as follows: (A,B) Vacuole, 100 kDa subunit of the vacuolar ATPase; endosome, Pep12p; ER, Dpm1p; Golgi, Sed5p; (C,D) early Golgi, Sec22; late Golgi, Kex2p. (E) Wild-type CJY090 and (F) CJY091 *drs2Δ* cells expressing Gea2-3xGFP from its chromosomal location were grown to mid-logarithmic phase and observed by fluorescence microscopy.

in the S100 fraction, and 36% in the P100; whereas in *drs2Δ* 63% was in the S100 and 37% in the P100 fraction. Overall, there did not appear to be a major difference in fractionation pattern between wild type and the *drs2Δ* mutant for the markers we tested (Fig. 3). In both cases, a vacuolar marker was found predominantly in the lighter fractions of the gradient (highest levels in fractions 3 and 4; Fig. 3A,B), whereas early Golgi and ER markers fractionated in the part of the gradient where denser membranes were located. In both wild type and *drs2Δ*, the endosomal marker Pep12 was clearly separated from other organelle markers, peaking in fraction 6 for the wild-type strain (Fig. 3A) and in fraction 7 for *drs2Δ* (Fig. 3B). The late Golgi marker Kex2p peaked in fraction 8 in both wild type and *drs2Δ* (Fig. 3C,D). The early Golgi markers were in denser membranes, with Sec22 peaking in fraction 10 (Fig. 3C,D). The ER markers Dpm1p and Sec61p had a somewhat broader profile than the Golgi markers, with the peak extending over fractions 9, 10 and 11 for wild type (Fig. 3A and data not shown) and in fractions 8, 9 and 10 for *drs2Δ (*Fig. 3B and data not shown). Interestingly, membranes containing the ER-Golgi SNARE Sed5p were the most dense, peaking in fraction 12 (Fig. 3A,B). The lack of good separation between ER and early Golgi markers shows the similarity in composition at this level of analysis between ER and Golgi membranes, and is consistent with the view that ER and Golgi membranes of yeast are not as distinct in composition as is the case for mammalian cells. The Gea2p protein overlapped extensively with Kex2p and had a similar profile, with the notable exception that a shoulder of the Gea2p peak extended to the denser fractions, where early Golgi membranes fractionate. For Kex2p, there was a predominance of the protein in lighter fractions compared to Gea2p. These results are consistent with a portion of Gea2p being localized to the Kex2p compartment, along with Drs2p, and another portion in earlier Golgi compartments.

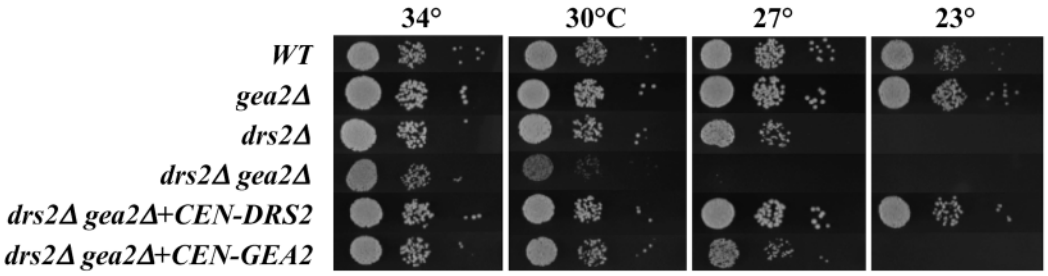

Fig. 4. A *drs2Δ gea2Δ* double mutant strain has a more severe cold-sensitive growth defect than a *drs2Δ* mutant alone. Strains SEY6210 (WT), CJY049-2-1 (*gea2Δ*), SEY6210 *drs2Δ::URA3* (*drs2Δ*) and SCY020-9-4 (*drs2Δ gea2Δ*) alone or carrying the indicated plasmids, were grown to stationary phase, and serial dilutions were spotted onto plates. Note that *drs2Δ gea2Δ* fails to grow at 27°C, a temperature at which *drs2Δ* grows well.

We next carried out fluorescence analysis to determine the distribution of Gea2p-GFP in wild-type and *drs2Δ* mutant cells. Both strains showed a pattern of spots typical of the yeast Golgi apparatus (Fig. 3E,F). The spots in the *drs2Δ* strain appeared to be somewhat weaker than those in wild type (Fig. 3E,F). These results, coupled with the fractionation results described above, indicate that Drs2p is not the sole localization determinant of Gea2p, but may contribute to Gea2p localization.

To further explore a functional link between Gea2p and Drs2p, we tested for genetic interactions. Neither *DRS2* nor *GEA2* is essential, although *drs2Δ* has cold sensitive growth and trafficking defects (Chen et al., 1999). *gea2Δ* has no observable growth defect and secretion is not delayed in this mutant (Peyroche et al., 2001). Interestingly, it has been shown previously that *gea2Δ*, like *drs2Δ*, is synthetically lethal with *arf1Δ*, whereas *gea1Δ arf1Δ* is viable (Spang et al., 2001). The *drs2Δ gea2Δ* double mutant is viable, but clearly has a more severe cold-sensitive growth defect than *drs2Δ* alone (Fig. 4). This genetic interaction between *DRS2* and *GEA2* suggests that Drs2p and Gea2p functionally interact in yeast cells.

The C-terminal region of Drs2p is essential for its function

As shown above, we found that the Gea2p Sec7 domain interacts with a 75 amino acid region present in the C-terminal cytoplasmic domain of Drs2p. To further map the Gea2p binding site on Drs2p, we carried out a reverse two-hybrid screen. We randomly mutagenized the 2-hybrid construct containing the C-terminal region of Drs2p identified in the original screen (amino acids 1230-1355), and looked for point mutants that abolished interaction with the Gea2p Sec7 domain. All such mutants had at least one substitution in a 21-amino-acid region (amino acids 1250-1270; Fig. 5A). This region is highly conserved among fungal homologues of Drs2p, and is just upstream of a region highly conserved among all, including mammalian, Drs2p homologues (Fig. 5A).

We carried out a deletion analysis to determine if the C-terminal tail of Drs2p is required for its function. Truncations up to amino acid 1283 were able to fully complement the cold-sensitive growth defect of *drs2*Δ (Fig. 5B, Δ1283-1355). This result indicates that the two NPFXD motifs, potential binding sites for the Pan1/End3/Sla1 complex (Howard et al., 2002; Tan et al., 1996), and half of the highly conserved domain are not required for full function of Drs2p. However, the additional removal of the GFAFSQAEE sequence (Δ1274-1355) strongly abrogated complementation. Further deletion of 15 amino acids into the Gea2 binding domain completely abolished complementation. We constructed internal deletions encompassing either the GFAFSQAEE motif, the upstream 15 amino acids impinging into the Gea2 binding region, or both. The construct removing both regions was completely unable to complement the cold-sensitive growth defect of *drs2Δ*, indicating that this region is essential for the function of Drs2p (Fig. 5B). Deletion of the GFAFSQAEE region severely compromised function, whereas deletion of the upstream 15 amino acids had only a mild effect (Fig. 5B). These results suggest that the Gea2p binding region may contribute to this function, although it cannot be ruled out that deletion into the adjacent Gea2p binding region of Drs2p is simply exacerbating the essential function of the highly conserved region. Surprisingly, a deletion of most of the Gea2 binding domain, as defined by the reverse two-hybrid screen, had no effect on complementation (Fig. 5B, deletion 1250-1263). However, overexpression of *GEA1* or *GEA2* improves the growth of strains carrying poorly complementing deletions (Fig. 5B), and we have demonstrated a genetic interaction between *GEA2* and *DRS2* (see Fig. 4). Thus, while Gea2p binding may not be essential for Drs2p function, these data suggest that the interaction between Drs2p and Gea2p contributes to the role Drs2p plays in trafficking.

To address the possibility that the mutant proteins that failed to complement were unstable, we performed western analysis. The internal deletion mutants were expressed to nearly the same level as wild-type Drs2p. The truncation mutants ranged from 10-50% wild-type level although the level of protein did not correlate with the ability to complement. In addition, differential centrifugation experiments indicated that the mutant proteins were not appreciably mislocalized (data not shown). Another possible explanation for the lack of complementation is that the C-terminal truncations perturbed the ATPase activity of Drs2p, which is known to be essential for its function. If this is the case, then co-expression of an ATPase-defective mutant of Drs2p along with a C-terminal truncation should also fail to complement the growth defect of Drs2p since neither protein would provide a functional ATPase activity. We performed this experiment using the *drs2-D560N* mutant that is completely defective in ATPase activity (Chen et al., 1999). Co-expression of this ATPase-defective mutant and the *drs2Δ1246-1355* truncation (the least stable truncation mutant) resulted in growth of *drs2Δ* cells at the non-permissive temperature (Fig. 5C), indicating that Drs2p C-terminal truncation mutants can provide ATPase activity. This intragenic complementation also suggests that the ATPase and C-terminal domains perform two independent and essential functions for Drs2p.

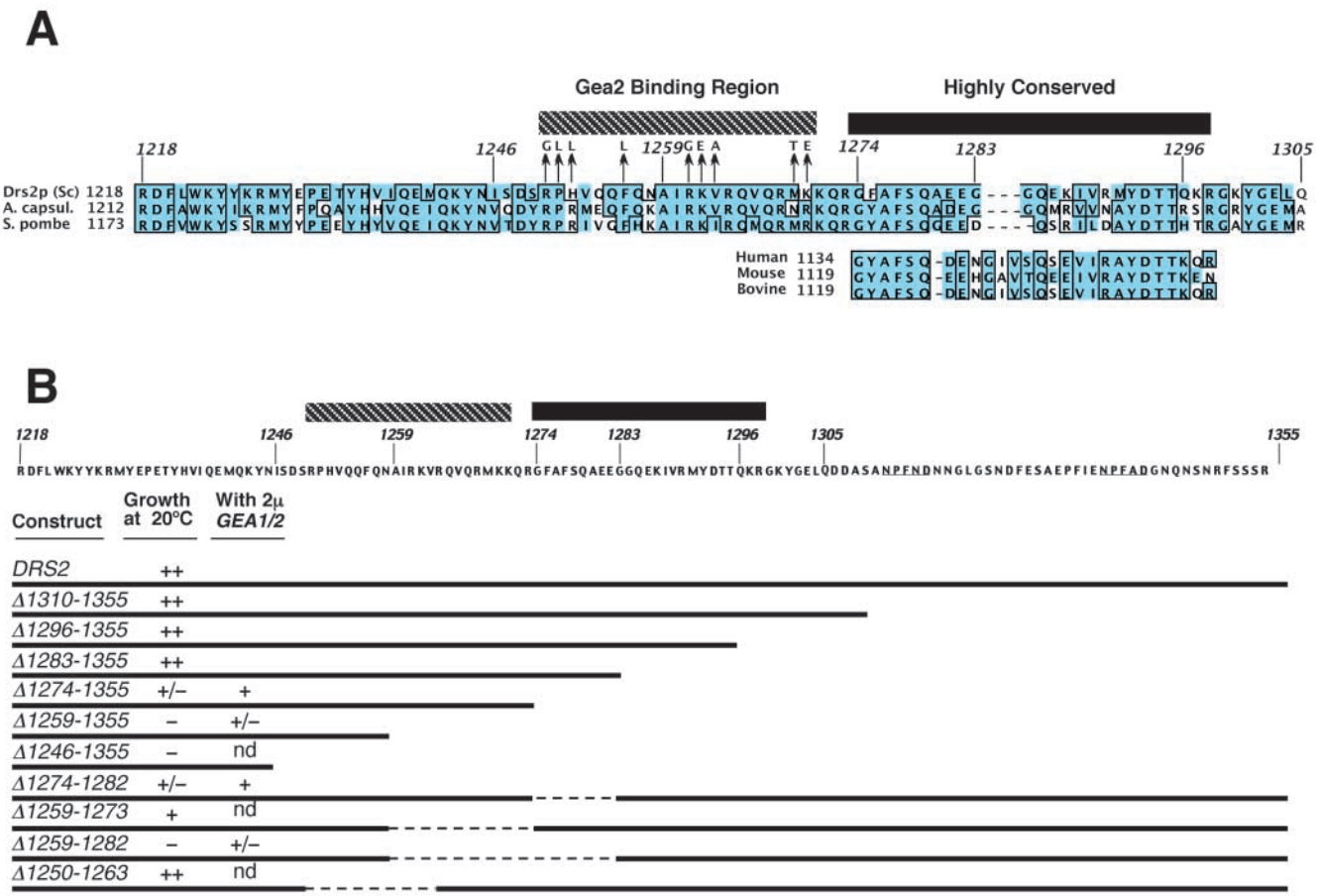

Fig. 5. The C-terminal region of Drs2p is essential for its function. (A) Sequence alignment of the entire C-terminal cytoplasmic region of *Saccharomyces cerevisiae* (Sc) Drs2p (accession number NP_009376) and its homologues from *Ajellomyces capsulatus* (accession number AAF90186) and *Schizosaccharomyces pombe* (accession number NP_596486). Also shown is an alignment of a region conserved between mammalian and yeast ATPases. (B) C-terminal truncations and internal deletions of Drs2p were transformed into SEY6210 *drs2Δ::TRP1*, and ability to grow at 20°C was determined. Truncations or deletion mutants that failed to grow at 20°C were transformed with multicopy plasmids carrying *GEA1* and *GEA2*, and growth was monitored at 20°C. In each case, overexpression of either Gea1p or Gea2p partially suppressed the growth defect. Hatched box, Gea2p interaction region; black box, highly conserved region; underlined, NPFXD motifs. (C) SEY6210 *drs2Δ::TRP1* was co-transformed with low-copy centromeric plasmids carrying *drs2-D560N* and the C-terminal truncation mutant *drs2Δ1246-1355* (lower panel), and appropriate vector controls (upper panel). Some variability in the level of growth of the four independently isolated *drs2-D560N* + *drs2Δ1246-1355* co-transformants at the non-permissive temperature was noted, but in all cases significant growth, compared to a *drs2Δ* strain, was evident.

Mutations in Gea2p that inhibit interaction with Drs2p are important for function

We carried out reverse two-hybrid analysis to map the interaction domain of Drs2p on Gea2p. Mutations that perturbed the interaction were clustered in the C-terminal third of the Sec7 domain, including the single mutants V698G, I705T, C733G and C733R, and the double mutants R643G S697P and Y627H F665S. In addition, deletion of the C-terminal 13 amino acids of the Sec7 domain (amino acids 755-766) abolished interaction in the two-hybrid assay (Fig. 6A and data not shown). These mutations are located relatively close to each other on the crystal structure of the Gea2 Sec7 domain

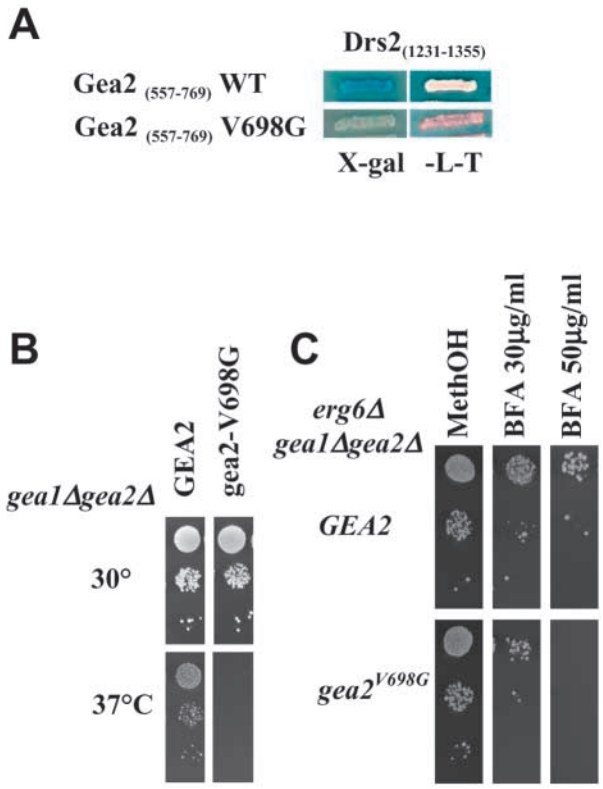

Fig. 6. The *gea2-V698G* mutant fails to interact with Drs2p, and is temperature and BFA-sensitive. (A) Strain Y190 carrying the C-terminal region of Drs2p (amino acids 1230-1355) in the two-hybrid prey plasmid and either the wild-type Gea2 or *gea2-V698G* mutant Sec7 domain as the bait plasmid were grown on medium containing X-gal (left) or on control medium (right). (B) Strains CJY092 *gea1Δ gea2Δ/pSKP1 (pCEN-GEA2)* and CJY093 *gea1Δ gea2Δ/pCEN-gea2-V698G* were grown to stationary phase and serial dilutions spotted onto plates grown either at 30°C or 37°C. (C) Strains CJY092 *gea1Δ gea2Δ/pSKP1(pCEN-GEA2)* and CJY093 *gea1Δ gea2Δ/pCEN- gea2-V698G* were grown to stationary phase and serial dilutions spotted onto plates containing 30 or 50 μg/ml BFA or solvent alone (methanol). Plates were incubated at 30°C.

(Goldberg, 1998). We introduced the Y627H, R643G, F665S, S697G, V698G, I705T and C733R mutations into Gea2p expressed from a low-copy centromeric plasmid. A plasmid shuffling approach in a *gea1Δ gea2Δ* strain was used to test whether each mutant could support growth of the cells. The *gea1Δ gea2Δ* cells expressing *gea2-Y627H*, *gea2-F665S* or *gea2-V698G* were thermosensitive, failing to grow at or above 37°C (Fig. 6B and data not shown). We carried out western analysis on the two-hybrid fusions carrying the Y627H, R643G, F665S, S697G, V698G, I705T and C733R mutations of Gal4BD-Gea1p, to compare the expression level at permissive temperature and after incubation for 1.5 hours at 38°C. The *gea2-V698G* mutant clearly was expressed at the same level as in a wild-type strain at both temperatures, so the loss of interaction and thermosensitive phenotype are not due to instability of the protein. In addition, the *gea2-V698G* mutant retained the ability to interact with at least one other Gea2p two-hybrid partner (data not shown). Western analysis of full-length gea2-V698Gp also showed that it was expressed at normal levels in yeast cells. The *gea2-V698G* mutant was tested further, and found to be hypersensitive to brefeldin A (BFA) (Fig. 6C). Interestingly, the region of Gea2p that is involved in interaction with Drs2p overlaps a region of Sec7 domains previously shown to be involved in BFA sensitivity and resistance (Peyroche et al., 1999). These results demonstrate that the region of Gea2p that interacts with Drs2p is important for its function.

We carried out pulse-chase analysis to determine whether *gea2-V698G* has a secretion defect. Strains deleted for *GEA1* and *GEA2* at their chromosomal locations (*gea1Δ gea2Δ*), and carrying either wild type *GEA2* or *gea2-V698G* on a low-copy centromeric (CEN) plasmid were examined. Total secretion of proteins into the medium was monitored at the non-permissive temperature of 38°C. In contrast to the previously characterized *gea1-4 gea2Δ* and *gea1-6 gea2Δ* temperature-sensitive mutants, the *gea2-V698G* mutant did not manifest a glycosylation defect, and did not have a cargo-specific secretion defect (Fig. 7A). Transport of the vacuolar hydrolase carboxy-peptidase Y (CPY) was slowed but not blocked at all temperatures tested (Fig. 7B). There was a slight accumulation of the p1 precursor form, found in the ER and early Golgi compartments, but not of the p2 late Golgi precursor form, indicating a slowing of transport from the ER to the Golgi and/or though early Golgi compartments. We also examined a secreted protein, the mating pheromone alpha-factor, using pulse-chase analysis. In this case, no defect in secretion or in Kex2-mediated processing was observed in the *gea2-V698G* mutant compared to wild type (data not shown).

gea2-V698G cells were prepared for electron microscopy using the reduced osmium fixation method and counterstaining with thiocarbohydrazide-silver proteinate. This method results in a staining gradient from the lightly stained ER/nuclear envelope, to the darkly stained secretory granules/vesicles and cell wall, as described previously (Rambourg et al., 2001). Strains deleted for *GEA1* and *GEA2* at their chromosomal locations (*gea1Δ gea2Δ*), and carrying either wild-type *GEA2* or *gea2-V698G* on a low-copy centromeric plasmid were examined. The *gea1Δ gea2Δ/pCEN-GEA2* strain had a phenotype similar to wild type, although it clearly showed mild morphological defects along the secretory pathway (Fig. 8A,B). This phenotype is caused by the *GEA1* deletion. Tubular networks in which secretory vesicles/granules were segregating appeared normal. It was possible to find cells that contained numerous secretory vesicles/granules in the bud (Fig. 8B), as has been described for wild-type cells (Rambourg et al., 2001). In the *gea2-V698G* mutant, a number of aberrant morphological features were noted. A fraction of cells (approximately 5-10%) showed large accumulations of aberrant membranes, which have the morphology and staining properties of the ER (Fig. 8C). In contrast to wild-type cells, *gea2-V698G* cells did not have accumulations of homogeneously sized vesicles in growing buds. Instead, small numbers of secretory vesicles/granules were present in or near buds, many of them smaller than those seen in control cells (Fig. 8D, arrowheads). Elsewhere in the cell, more secretory vesicles/granules than normal were found scattered throughout the cytoplasm (Fig. 8D, arrowheads). Cells in which secretory vesicles/granules were segregating in abnormal membrane structures were frequent (Fig. 9AB, arrows). In wild-type cells, secretory granules/vesicles form within tubular network structures (Rambourg et al., 2001), whereas in the *gea2-V698G*

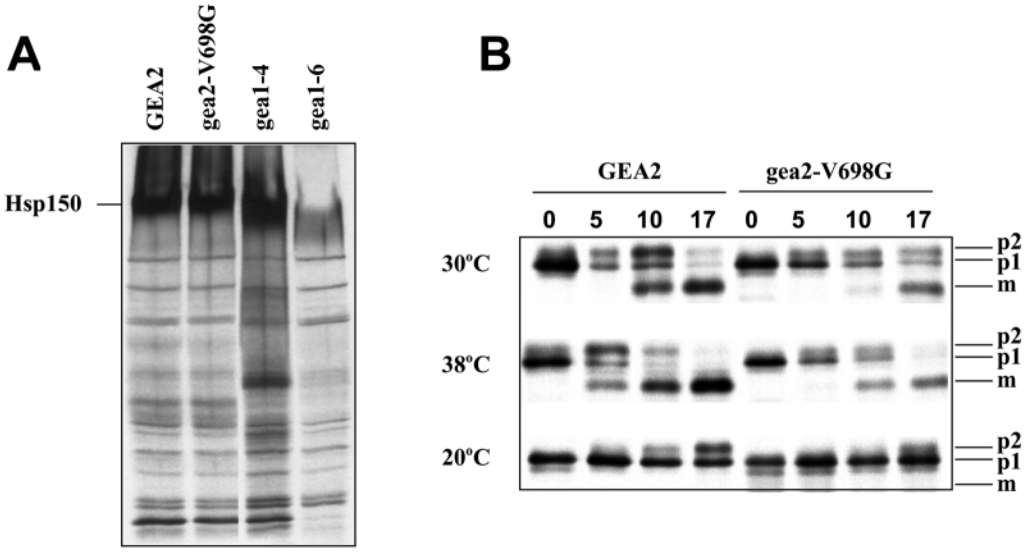

Fig. 7. Trafficking phenotype of the *gea2-V698G* mutant. Strains CJY092 *gea1Δgea2Δ/pSKP1(pCEN-GEA2)* and CJY093 *gea1Δgea2Δ/pCEN-gea2-V698G* were grown to exponential phase and incubated for 1 hour at 38°C, pulse-labeled for 10 minutes with [^{35}S]methionine/cysteine, then chased with non-radioactive amino acids for 30 minutes, all at 38°C. (A) Proteins secreted into the medium were recovered and analyzed as described in Materials and Methods. Strains CJY062-10-3 *gea1-4 gea2Δ* and APY022 *gea1-6 gea2Δ* (Peyroche et al., 2001) were treated similarly and included as controls. (B) Strains listed above were grown at 30°C and shifted to the indicated temperature for 1 hour before labeling for 5 minutes. Cell lysates were prepared at the chase times indicated and immunoprecipitated with anti-CPY antibodies. The ER-early-Golgi localized p1 precursor, late-Golgi p2 precursor, and mature (m) forms of CPY are indicated. Note that at 20°C, transport through the secretory pathway is significantly slowed, and no mature CPY accumulates during the short time course of this experiment.

mutant, forming secretory granules (Fig. 9A,B, arrowheads) were found in abnormally fenestrated (Fig. 9A) or unfenestrated (Fig. 9B) membrane structures. We also examined *drs2Δ* cells after incubation for 1 hour at a semi-permissive temperature (24°C). We noted a marked reduction in the number of Golgi tubular networks in *drs2Δ* cells compared to the wild-type cells grown at 24°C (Fig. 9C and data not shown). As has been described previously for *drs2Δ* cells (Chen et al., 1999), we observed accumulation of unfenestrated spherical structures, as well as spherical structures made up of abnormally fenestrated membrane (Fig. 9C,D). Similar to what was found in the *gea2-V698G* mutant, we observed forming secretory granules in abnormally fenestrated or unfenestrated membrane structures (Fig. 9E, arrow). These results demonstrate that *gea2-V698G* and *drs2Δ* are defective in the membrane transformation events that lead to segregation of secretory granules/vesicles.

Discussion

The Gea1p and Gea2p proteins are guanine nucleotide exchange factors (GEFs) for the small GTPase Arf. The Gea1p and Gea2p proteins are 50% identical and are functionally redundant: individual deletion of *GEA1* or *GEA2* has no growth or secretion defect detected to date, but a *gea1Δ gea2Δ* strain is inviable (Peyroche et al., 1996). Analysis of *gea1-ts gea2Δ* mutants has demonstrated a role for these ARF GEFs in transport through the Golgi apparatus and in maintenance of Golgi structure in *Saccharomyces cerevisiae* (Peyroche et al., 2001). Drs2p was identified in a synthetic lethal screen using *arf1Δ ARF2* (Chen and Graham, 1998). In yeast, there are two genes encoding Arf, with *ARF1* responsible for production of 90% of total Arf protein in cells and *ARF2* encoding only 10% (Stearns et al., 1990). Hence a cell with a deletion of *ARF1* expresses only about 10% of the normal level of Arf, and has both growth and secretion defects (Gaynor et al., 1998). The synthetic lethal screen with *arf1Δ* uncovered a number of mutations affecting clathrin function in yeast, suggesting that transport steps involving clathrin are the most sensitive to decreased levels of Arf (Chen and Graham, 1998). Interestingly, it has been reported that a *gea1Δarf1Δ* strain is viable, whereas *gea2Δarf1Δ* cells are non-viable (Spang et al., 2001), which might suggest a preferential role for Gea2p in clathrin function in yeast. Drs2p co-localizes with the Kex2p protease, and is required for clathrin-mediated sorting events at the late Golgi (Chen et al., 1999; Gall et al., 2002). Drs2p is predicted to be an amino-phospholipid translocase (or 'flippase'), and is one member of a family of five putative flippases in *Saccharomyces cerevisiae* (Hua et al., 2002; Pomorski et al., 2003).

In this work, we have demonstrated a direct interaction between Gea2p and Drs2p. We mapped the region of interaction in Gea2p to the C-terminal third of the Sec7 domain, and the region of interaction in Drs2p to a 20-amino acid region of the C-terminal cytoplasmic tail. This region is not well conserved among the four homologues of Drs2p in *Saccharomyces cerevisiae*, although there is some weak homology to the same region of Dnf1p. Hence it is possible that the difference in phenotypes between *drs2Δ* and *gea2-V698G*, a mutation that abolishes interaction with Drs2p, is due to the capacity of Gea2p to interact with Dnf1p, and perhaps other Drs2p homologues, in yeast.

Using fractionation analysis, we have demonstrated that a portion of Gea2p co-localizes with Kex2p, where Drs2p also localizes. There is a subpopulation of Gea2p that associates with early Golgi compartments, as has been demonstrated previously by co-immunolocalization experiments (Chantalat et al., 2003). Hence Gea2p appears to have multiple membrane localization sites. A similar result was obtained for its mammalian homologue, GBF1, which localizes both to ER exit sites and to Golgi compartments (García-Mata et al., 2003; Zhao et al., 2002). Since Drs2p is a transmembrane domain

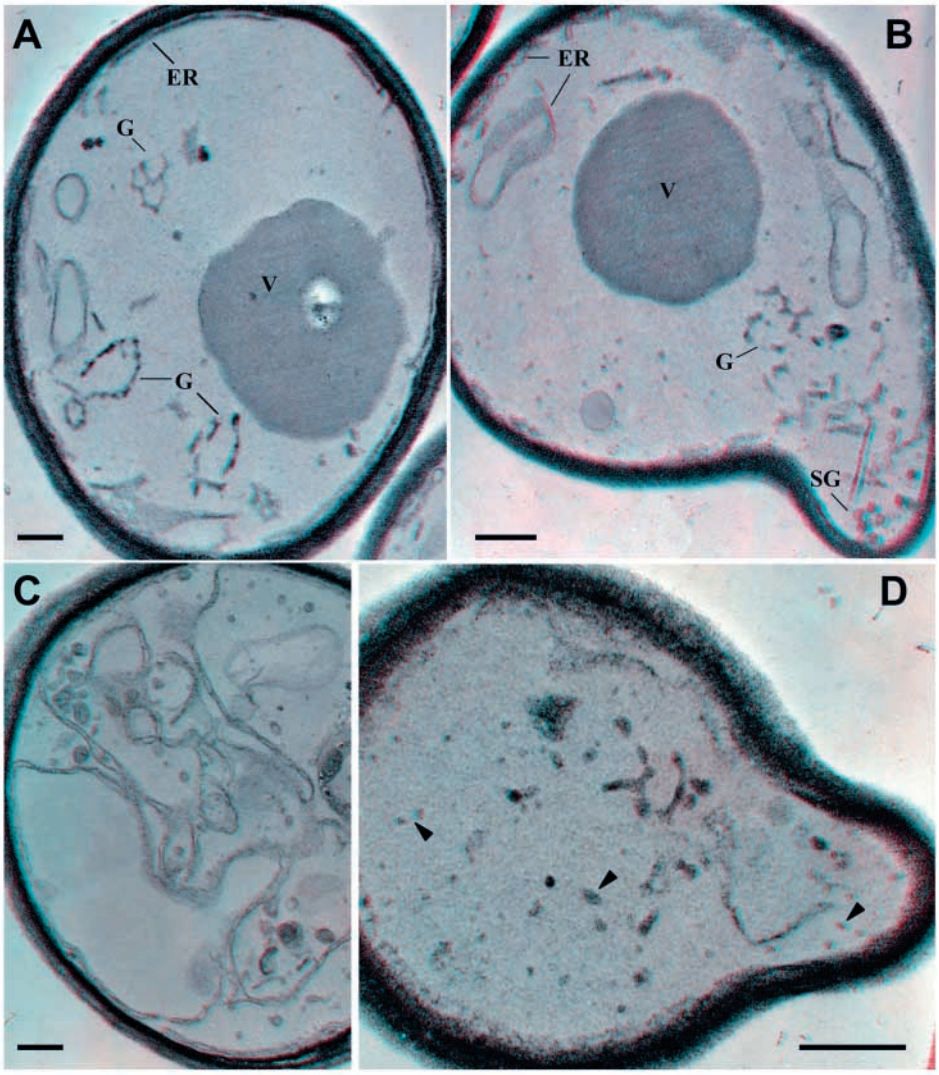

Fig. 8. Ultrastructural analysis of *gea2-V698G* and control cells grown to exponential phase at 24°C, then shifted for 1 hour to 38°C. Stereopairs of 0.20 μm thick sections of (A,B) CJY092 *gea1Δ gea2Δ/pCEN-GEA2* and (C-F) CJY093 *gea1Δ gea2Δ/pCEN-gea2-V698G* cells. ER, endoplasmic reticulum, G, Golgi, V, vacuole, SG, secretion granule/vesicle. (A) An image showing typical Golgi tubular network structures (G) scattered throughout the cytoplasm. (B) A cell with an emerging bud (lower right) with a typical accumulation of homogeneously sized secretion granules/vesicles (SG). (C) Cell showing abnormal accumulation of membranes throughout the cell. (D) Cell with an emerging bud lacking the normal accumulation of secretion granules/vesicles. Note the heterogeneous size and scattered distribution of secretion granules/vesicles (arrowheads). To view the 3D image of the structures, figures should be viewed through a pair of anaglyph (red-cyan) glasses with the red lens placed over the left eye. Scale bars: 0.5 μm.

protein, it is possible that it acts as a membrane receptor for Gea2p, which associates peripherally with membranes. Our data shows that if this is the case, Drs2p is not the only membrane receptor for Gea2p. Indeed, we have identified five additional transmembrane domain proteins in two-hybrid and genetic screens with Gea1p and Gea2p that are potential membrane receptors. We have characterized one of these transmembrane domain proteins, Gmh1p, and verified that it interacts with Gea2p in vivo (Chantalat et al., 2003). As is the case for *drs2Δ*, cells deleted for *GMH1* also show only a mild effect on Gea2p localization (Chantalat et al., 2003). The double mutant *drs2Δ gmh1Δ* is viable, and although there is an effect on Gea2p localization that is more severe than in either single mutant, some Gea2p is still able to bind to membranes (S.K.P. and C.L.J., unpublished results). We are testing the possibility that the other transmembrane-domain proteins identified in two-hybrid screens with Gea2p are also contributing to Gea2p localization. Hence, the mechanism by which the large Arf GEFs such as Gea2p are localized to membranes appears to be complex, with multiple membrane localization determinants each contributing to the steady-state localization of the protein in cells.

The phenotype of the *gea2-V698G* mutant, defective in its ability to interact with Drs2p, is consistent with a role for Gea2p in the formation of secretory granules/vesicles. It was previously shown that Drs2p is required for the formation of a class of secretory vesicles/granules that also requires clathrin, AP-1 and dynamin for their production (Gall et al., 2002; Gurunathan et al., 2002; Harsay and Schekman, 2002). The mechanism of formation of secretory granules/vesicles is highly conserved at the morphological level from yeast to mammalian cells (Rambourg et al., 2001). The first step is the fenestration of a saccular membrane, which then forms a tubular network with a hexagonal or pentagonal mesh. At the nodes of the meshes, material to be packaged into secretory vesicles/granules accumulates, as the surrounding tubular portions become gradually devoid of cargo. Eventually the tubules break to release the granule/vesicle into the cytoplasm (Rambourg et al., 2001).

As cargo molecules destined for secretion move through the Golgi apparatus, they are modified by glycosylation enzymes. The successive stages of the secretory pathway are defined by the action of the ordered series of modifications that a given cargo molecule undergoes (Brigance et al., 2000). The

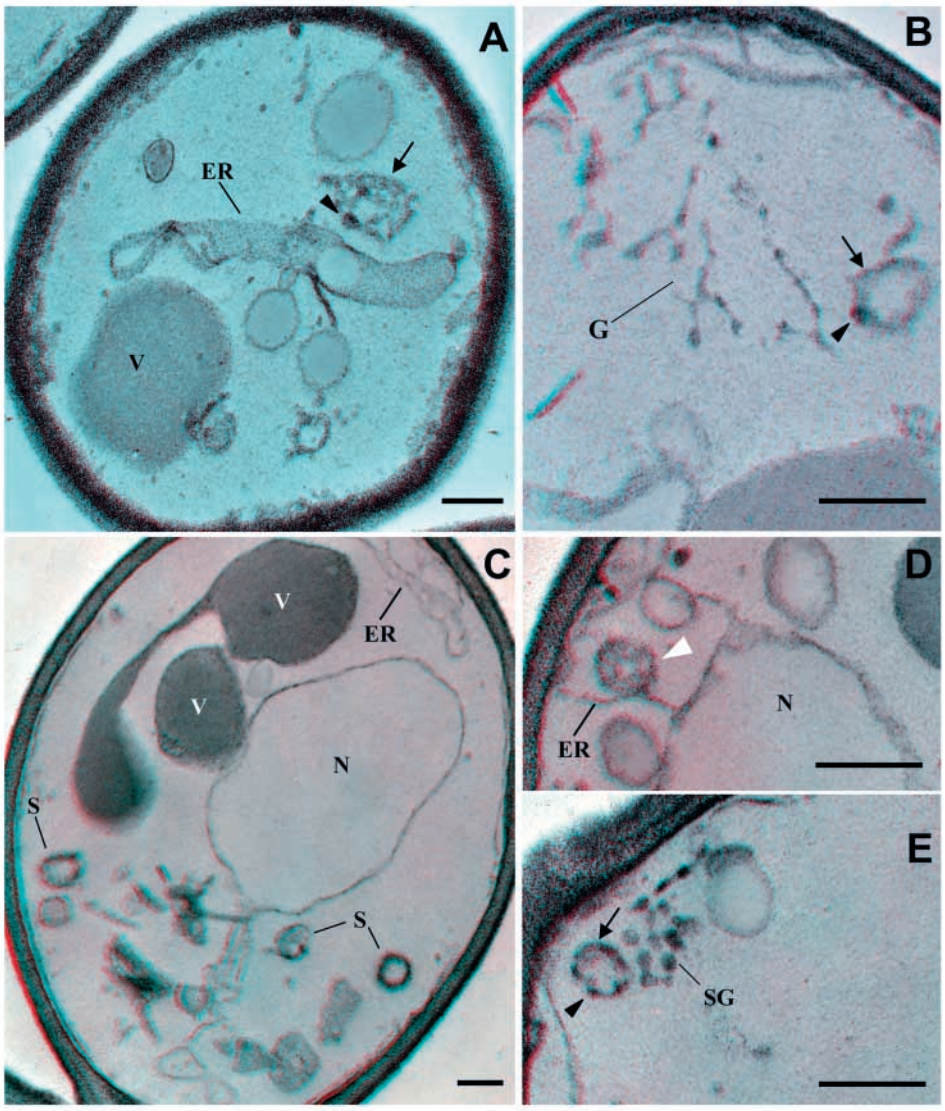

Fig. 9. (A,B) Stereopairs of 0.20 μm thick sections of CJY093 *gea1Δ gea2Δ/pCEN-gea2-V698G* cells prepared as described in Fig. 8. (A) Cell showing an abnormal Golgi element (arrow) with heterogeneously sized fenestrations and segregating granules (one indicated with an arrowhead). (B) Cell showing an abnormal Golgi element with almost no fenestrations (arrow) but nevertheless containing a segregating granule (arrowhead). (C-E) Strain SEY6210 *drs2Δ::URA3* was grown to exponential phase at 30°C, then shifted to 24°C for 1 hour. Stereopairs of 0.20 μm thick sections are shown. (C) Cell showing accumulation of spherical membrane structures (S) made up of unfenestrated membrane. (D) A higher magnification image of a spherical element made up of abnormally fenestrated membrane (white arrowhead). The element is connected to a ribbon of ER that, on the right, is continuous with the nuclear envelope. (E) Cell showing an abnormal Golgi element with almost no fenestrations (arrow) and containing segregating granules (one is marked by an arrowhead). ER, endoplasmic reticulum; G, Golgi; V, vacuole; SG, secretion granule/vesicle; S, spherical structure. To view the 3D image of the structures, figures should be viewed through a pair of anaglyph (red-cyan) glasses with the red lens placed over the left eye. Scale bars: 0.5 μm.

challenge now is to correlate this series of biochemical reactions with the morphological events of membrane fenestration, tubulation and granule formation. A first step towards this goal is to examine mutants with precisely defined lesions at the molecular level for their effects on the morphology of the secretory pathway. Our results suggest that Drs2p and Gea2p are involved in the processes of membrane fenestration and tubulation, early events in the morphological transformations that take place along the secretory pathway in yeast.

The *gea2-V698G* mutant accumulates aberrant ER membranes when grown at the non-permissive temperature, and shows defects in segregation of secretory granules very early in the process, with some granules forming in abnormally fenestrated membranes, and others forming in unfenestrated membranes. Most if not all secretory granules/vesicles observed in the *gea2-V698G* mutant have an abnormal morphology. The only trafficking defect we observed in *gea2-V698G* was a slowing of CPY transport in ER to early Golgi transport steps, consistent with the morphological observations. *drs2Δ* mutant cells have some features in common with the *gea2-V698G* mutant, with accumulation of unfenestrated membranes in which secretory granules are segregating. Abnormally fenestrated membranes are also observed, and the normal Golgi tubular networks are almost completely absent. However, in contrast to *gea2-V698G*, *drs2Δ* cells do have some secretory granules that appear normal. In *gea2-V698G* cells, despite the abnormal structure of secretory granules/vesicle and the elements that give rise to them, secretion of several proteins, including HSP150, the mating pheromone alpha-factor, and other proteins secreted into the medium, did not appear to be affected. Hence although the morphology of secretory granules/vesicles in this mutant is abnormal, they can function well enough to assure secretion of at least some proteins. Our results show that Gea2p, through its interaction with the Drs2p lipid-modifying enzyme, is involved in the morphological events of membrane fenestration and tubulation that lead to formation of secretory granules/vesicles.

We thank Gerry Waters and Randy Schekman for providing antibodies, M. Fromont-Racine and A. Jacquier for providing the yeast two hybrid library, Ben Glick, Chris Mullins and Gerald Peyroche for providing plasmids, and Sean Munro for providing the

C13-ABYS86 strain. S.C. was supported by a doctoral fellowship from the CEA and a fellowship from l'ARC (Association pour la Recherche contre le Cancer). This work was partially supported by a grant from the National Institutes of Health (GM62367) to T.R.G.

References

Brigance, W. T., Barlowe, C. and Graham, T. R. (2000). Organization of the yeast Golgi complex into at least four functionally distinct compartments. *Mol. Biol. Cell* **11**, 171-182.

Chantalat, S., Courbeyrette, R., Senic-Matuglia, F., Jackson, C. L., Goud, B. and Peyroche, A. (2003). A novel Golgi membrane protein is a partner of the ARF exchange factors Gea1p and Gea2p. *Mol. Biol. Cell* **14**, 2357-2371.

Chen, C. Y. and Graham, T. R. (1998). An arf1Delta synthetic lethal screen identifies a new clathrin heavy chain conditional allele that perturbs vacuolar protein transport in *Saccharomyces cerevisiae*. *Genetics* **150**, 577-589.

Chen, C. Y., Ingram, M. F., Rosal, P. H. and Graham, T. R. (1999). Role for Drs2p, a P-type ATPase and potential aminophospholipid translocase, in yeast late Golgi function. *J. Cell Biol.* **147**, 1223-1236.

Deitz, S. B., Rambourg, A., Kepes, F. and Franzusoff, A. (2000). Sec7p directs the transitions required for yeast Golgi biogenesis. *Traffic* **1**, 172-83.

Donaldson, J. G. and Jackson, C. L. (2000). Regulators and effectors of the ARF GTPases. *Curr. Opin. Cell Biol.* **12**, 475-482.

Flores, A., Briand, J. F., Gadal, O., Andrau, J. C., Rubbi, L., Van Mullem, V., Boschiero, C., Goussot, M., Marck, C., Carles, C. et al., (1999). A protein-protein interaction map of yeast RNA polymerase III. *Proc. Natl. Acad. Sci. USA* **96**, 7815-7820.

Gall, W. E., Geething, N. C., Hua, Z., Ingram, M. F., Liu, K., Chen, S. I. and Graham, T. R. (2002). Drs2p-dependent formation of exocytic clathrin-coated vesicles in vivo. *Curr. Biol.* **12**, 1623-1627.

García-Mata, R., Szul, T., Alvarez, C. and Sztul, E. (2003). ARF/COPI-dependent events at the ER-Golgi interface are regulated by the guanine-nucleotide exchange factor GBF1. *Mol. Biol. Cell* **14**, 2250-2261.

Gaynor, E. C., Chen, C. Y., Emr, S. D. and Graham, T. R. (1998). ARF is required for maintenance of yeast Golgi and endosome structure and function. *Mol. Biol. Cell* **9**, 653-670.

Geldner, N., Anders, N., Wolters, H., Keicher, J., Kornberger, W., Muller, P., Delbarre, A., Ueda, T., Nakano, A. and Jurgens, G. (2003). The Arabidopsis GNOM ARF-GEF mediates endosomal recycling, auxin transport, and auxin-dependent plant growth. *Cell* **112**, 219-230.

Goldberg, J. (1998). Structural basis for activation of ARF GTPase: mechanisms of guanine nucleotide exchange and GTP-myristoyl switching. *Cell* **95**, 237-248.

Gurunathan, S., David, D. and Gerst, J. E. (2002). Dynamin and clathrin are required for the biogenesis of a distinct class of secretory vesicles in yeast. *EMBO J.* **21**, 602-614.

Harsay, E. and Schekman, R. (2002). A subset of yeast vacuolar protein sorting mutants is blocked in one branch of the exocytic pathway. *J. Cell Biol.* **156**, 271-285.

Heinemeyer, W., Kleinschmidt, J. A., Saidowsky, J., Escher, C. and Wolf, D. H. (1991). Proteinase yscE, the yeast proteasome/multicatalytic-multifunctional proteinase: mutants unravel its function in stress induced proteolysis and uncover its necessity for cell survival. *EMBO J.* **10**, 555-562.

Howard, J. P., Hutton, J. L., Olson, J. M. and Payne, G. S. (2002). Sla1p serves as the targeting signal recognition factor for NPFX(1,2)D-mediated endocytosis. *J. Cell Biol.* **157**, 315-326.

Hua, Z., Fatheddin, P. and Graham, T. R. (2002). An essential subfamily of Drs2p-related P-type ATPases is required for protein trafficking between Golgi complex and endosomal/vacuolar system. *Mol. Biol. Cell* **13**, 3162-3177.

Jackson, C. L. (2004). The Sec7 family of Arf guanine nucleotide exchange factors. In *Arf Family GTPases* (ed. R. A. Kahn). Kluwer Academic Publishers (in press).

Jackson, C. L. and Casanova, J. E. (2000). Turning on ARF: the Sec7 family of guanine-nucleotide-exchange factors. *Trends Cell Biol.* **10**, 60-67.

Jackson, T. R., Kearns, B. G. and Theibert, A. B. (2000). Cytohesins and centaurins: mediators of PI 3-kinase-regulated Arf signaling. *Trends Biochem. Sci.* **25**, 489-495.

Longtine, M. S., Mckenzie, A., Demarini, D. J., Shah, N. G., Wach, A., Brachat, A., Philippsen, P. and Pringle, J. R. (1998). Additional modules for versatile and economical PCR-based gene deletion and modification in *Saccharomyces cerevisiae*. *Genetics* **14**, 953-961.

Mullins, C. and Bonifacino, J. S. (2001). Structural Requirements for Function of Yeast GGAs in Vacuolar Protein Sorting, α-Factor Maturation, and Interactions with Clathrin. *Mol. Biol. Cell* **21**, 7981-7994.

Peyroche, A., Paris, S. and Jackson, C. L. (1996). Nucleotide exchange on ARF mediated by yeast Gea1 protein. *Nature* **384**, 479-481.

Peyroche, A., Antonny, B., Robineau, S., Acker, J., Cherfils, J. and Jackson, C. L. (1999). Brefeldin A acts to stabilize an abortive ARF-GDP-Sec7 domain protein complex: involvement of specific residues of the Sec7 domain. *Mol. Cell* **3**, 275-285.

Peyroche, A., Courbeyrette, R., Rambourg, A. and Jackson, C. L. (2001). The ARF exchange factors Gea1p and Gea2p regulate Golgi structure and function in yeast. *J. Cell Sci.* **114**, 2241-2253.

Pomorski, T., Lombardi, R., Riezman, H., Devaux, P. F., Van Meer, G. and Holthuis, J. C. (2003). Drs2p-related P-type ATPases Dnf1p and Dnf2p Are Required for Phospholipid Translocation across the Yeast Plasma Membrane and Serve a Role in Endocytosis. *Mol. Biol. Cell* **14**, 1240-1254.

Rambourg, A. and Clermont, Y. (1990). Three-dimensional electron microscopy: structure of the Golgi apparatus. *Eur. J. Cell Biol.* **51**, 189-200.

Rambourg, A., Jackson, C. L. and Clermont, Y. (2001). Three dimensional configuration of the secretory pathway and segregation of secretion granules in the yeast *Saccharomyces cerevisiae*. *J. Cell Sci.* **114**, 2231-2239.

Randazzo, P. A., Miura, K., Nie, Z., Orr, A., Theibert, A. B. and Kearns, B. G. (2001). Cytohesins and centaurins: mediators of PI 3-kinase regulated Arf signaling. *Trends Biochem. Sci.* **26**, 220-221.

Robinson, M. S. and Bonifacino, J. S. (2001). Adaptor-related proteins. *Curr. Opin. Cell Biol.* **13**, 444-453.

Schoepfer, R. (1993). The pRSET family of T7 promoter expression vectors for Escherichia coli. *Gene* **14**, 83-85.

Sherman, F., Fink, G. R. and Lawrence, C. W. (1979). Methods in Yeast Genetics: A Laboratory Manual. Cold Spring Harbor, N.Y.: Cold Spring Harbor Laboratory.

Spang, A., Herrmann, J. M., Hamamoto, S. and Schekman, R. (2001). The ADP ribosylation factor-nucleotide exchange factors Gea1p and Gea2p have overlapping, but not redundant functions in retrograde transport from the Golgi to the endoplasmic reticulum. *Mol. Biol. Cell* **12**, 1035-1045.

Stearns, T., Kahn, R. A., Botstein, D. and Hoyt, M. A. (1990). ADP ribosylation factor is an essential protein in *Saccharomyces cerevisiae* and is encoded by two genes. *Mol. Cell. Biol* **10**, 6690-6699.

Tan, P. K., Howard, J. P. and Payne, G. S. (1996). The sequence NPFXD defines a new class of endocytosis signal in *Saccharomyces cerevisiae*. *J. Cell Biol.* **135**, 1789-1800.

Tang, X., Halleck, M. S., Schlegel, R. A. and Williamson, P. (1996). A subfamily of P-type ATPases with aminophospholipid transporting activity. *Science* **272**, 1495-1497.

Zhao, X., Lasell, T. K. and Melancon, P. (2002). Localization of large ADP-ribosylation factor-guanine nucleotide exchange factors to different Golgi compartments: evidence for distinct functions in protein traffic. *Mol. Biol. Cell* **13**, 119-133.